

A Series-LC-Filtered Active Damper for AC Power Electronics Based Power Systems

Wang, Xiongfei; Blaabjerg, Frede; Loh, Poh Chiang; Pang, Ying

Published in:

Proceedings of the 30th Annual IEEE Applied Power Electronics Conference and Exposition, APEC 2015

DOI (link to publication from Publisher):

[10.1109/APEC.2015.7104397](https://doi.org/10.1109/APEC.2015.7104397)

Publication date:

2015

Document Version

Early version, also known as pre-print

[Link to publication from Aalborg University](#)

Citation for published version (APA):

Wang, X., Blaabjerg, F., Loh, P. C., & Pang, Y. (2015). A Series-LC-Filtered Active Damper for AC Power Electronics Based Power Systems. In *Proceedings of the 30th Annual IEEE Applied Power Electronics Conference and Exposition, APEC 2015* (pp. 506-512). IEEE Press.
<https://doi.org/10.1109/APEC.2015.7104397>

General rights

Copyright and moral rights for the publications made accessible in the public portal are retained by the authors and/or other copyright owners and it is a condition of accessing publications that users recognise and abide by the legal requirements associated with these rights.

- Users may download and print one copy of any publication from the public portal for the purpose of private study or research.
- You may not further distribute the material or use it for any profit-making activity or commercial gain
- You may freely distribute the URL identifying the publication in the public portal -

Take down policy

If you believe that this document breaches copyright please contact us at vbn@aub.aau.dk providing details, and we will remove access to the work immediately and investigate your claim.

A Series- LC -Filtered Active Damper for AC Power Electronics Based Power Systems

Xiongfei Wang, Poh Chiang Loh, Frede Blaabjerg
Department of Energy Technology, Aalborg University
Aalborg, Denmark
xwa@et.aau.dk, pcl@et.aau.dk, fbl@et.aau.dk

Ying Pang
KK Wind Solutions a/s
Ikast, Denmark
yipan@kkwindsolutions.com

Abstract—This paper proposes an active damper with a series LC -filter for suppressing resonances in an ac power electronics based power system. The added filter capacitor helps to lower the voltage stress of the converter to be used for implementing the damper. Unlike active filters for the compensation of low-order harmonics, the proposed active damper deals with the resonances caused by the interactions among grid-connected converters and reactive elements of the system, which are higher-order and vary in a wide frequency range. To confirm the validity of the damper, a three-phase experimental system is built, where the damper is integrated into a grid-connected converter. The results obtained from the experiments demonstrate the stability enhancement of ac power electronics based power systems by the active damper.

Keywords—Stability, resonance, power electronics based power systems, active damper

I. INTRODUCTION

More ac power electronics based power systems are being built in the future, due to the increasing use of power electronic converters for renewable power sources and energy-efficient loads [1], [2]. They are characterized with full controllability, sustainability, and improved efficiency, but they also bring in wideband harmonics by the nonlinear switching operation of converters [3]–[5]. Those harmonics may trigger the resonance frequencies residing in the reactive components, such as power cables, passive filters, and power factor correction capacitors [6], [7]. Such resonance frequencies may further interact with the control loops of converters, leading to harmonic instability phenomena in a wide frequency range [7]–[9].

There are, in general, two major approaches for stabilizing power electronics based power systems [9]–[16]. The one is to re-shape the dynamic properties of the converters by adding control loops or digital filters into the control system [9]–[11]. Lossless damping can thus be attained, yet their effectiveness is usually affected by the dynamics of other converters and the system conditions [9]. The other type is to employ additional devices, either passive or active, as dampers for stabilizing the systems [12]–[16]. Passive dampers generally achieve a robust damping, but additional losses are inevitable [12], [13]. Active dampers with the reduced losses are thus preferred [14]–[16], which are based on a converter with a high control bandwidth,

for selectively damping those high-frequency resonances in the power systems [14]–[16].

In [14], the active damper is used in parallel with other grid converters at the Point of Common Coupling (PCC) of an ac system. By dynamically shaping the equivalent grid impedance at the PCC, the active damper mitigates instabilities effectively. Compared to conventional active filters for low-order harmonic resonance damping [17], [18], the active damper in [14] has the same circuit topology. Yet it focuses only on high-frequency resonances from 600 Hz to 2 kHz, which allows a lower rated power for the active damper. However, it requires switching at a higher frequency than the normal source and load converters, in order to provide the necessary bandwidth of the damping. This requirement is costly for the active damper in [14], since the high-bandwidth current flow causes the higher voltage drop across the series ac L -filter [14]–[15], which imposes a higher voltage rating on the active damper.

To further reduce the voltage stresses imposed on the active damper, a series LC -filtered active damper is proposed in this paper. An extra ac capacitor is added in series for withstanding most of the system voltage. Thus, the converter implemented for active damper can then be designed with a lower voltage rating and a smaller inductor. This LC -filtered active damper is, no doubt, similar to the hybrid active filters developed in [19]. Yet their control requirements and challenges encountered are significantly different with the active damper concentrating on higher-frequency resonance damping, rather than the low-order harmonic suppression targeted by active filters. Moreover, the varying system resonance frequency complicates the design of the LC filter and controller for active damper. To confirm the validity of the system design, a three-phase laboratory setup is built and tested, where the active damper is implemented to stabilize the interaction between the grid impedance and the current control of a common LCL -filtered grid converter. Experimental results demonstrate the effectiveness of the series- LC -filtered active damper developed in this work.

II. OPERATION PRINCIPLE

A. System Description

Fig. 1 shows an ac power electronics based power system with the proposed series LC -filtered active damper added at the PCC of multi-paralleled, LCL -filtered grid converters. In such a system, there are main two types of resonances:

This work was supported by European Research Council (ERC) under the European Union's Seventh Framework Program (FP/2007-2013)/ERC Grant Agreement [321149-Harmony].

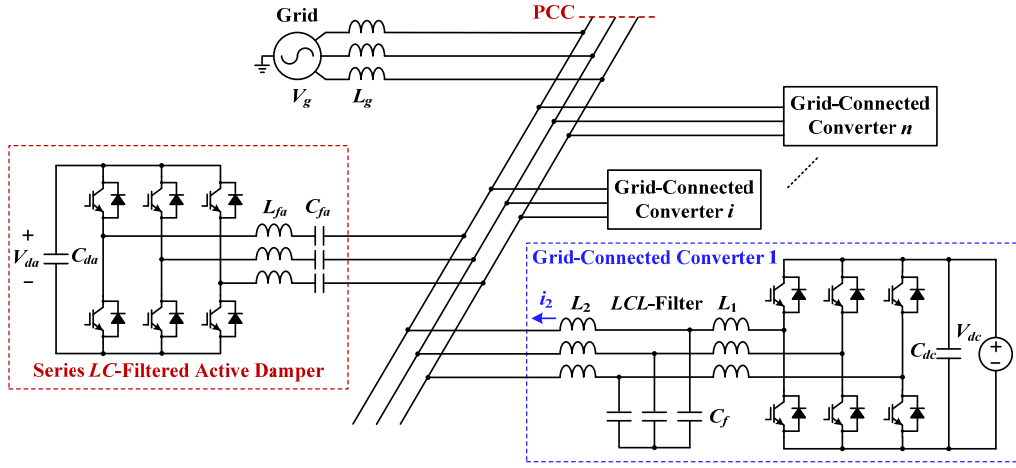


Fig. 1. An ac power electronics based power system with the series-LC-filtered active damper and multiple paralleled LCL-filtered grid converters.

1) *Sub-synchronous resonances*: They are mainly resulted from the interactions among the outer power control and grid synchronization loops of grid converters [20]-[22]. It has been shown that the constant power control loops and Phase-Locked Loop (PLL) may lead to the negative output resistances below the grid fundamental frequency, owing to their low bandwidth [20]. The negative resistances may destabilize the system with sub-synchronous oscillations.

2) *Super-synchronous resonances*: These resonances above the fundamental frequency can be triggered by grid background harmonics, which are mainly low-order (5th and 7th) [4]-[6], or caused by the interactions among current control loops of grid converters, which is typically in a high-frequency range (600 Hz - 2 kHz) [7]-[9], [23]-[25]. The latter phenomenon is also known as the harmonic instability [7], or electrical resonance instability [24], in order to distinguish it from the resonances formed merely by the passive components of the system.

Similarly to the transformerless hybrid active filter in [19], the added filter capacitor C_{fa} is used for withstanding most of the PCC voltage, thereby allowing a lower rated voltage and a smaller filter inductor L_{fa} to be used, in turn. However, the active filter is mainly used to mitigate dominant low-frequency harmonics. Its control performances are therefore less stringent. LC-filter resonance frequency of the active filter is also usually tuned close to the low-order harmonics, which is different from an active damper.

Two important aspects should be taken into account in the design of series LC-filter for the active damper. First, the filter exhibits a capacitive characteristic at those frequencies below the resonance frequency formed by C_{fa} and L_{fa} . It restricts the immediate use of usual integral controllers, which demands the inductive characteristic between a voltage-source converter and the grid [26]. Second, C_{fa} affects the power transfer capability of the active damper and the expected dc-link voltage [27]. L_{fa} is dependent on the output current ripple of damping converter. In this work, the resonance frequency of C_{fa} and L_{fa} is designed slightly lower than the smallest system resonance frequency¹.

¹ Filter resonance relates to C_{fa} and L_{fa} of the active damper only, while system resonance relates to all reactive elements and converter impedances found in the system.

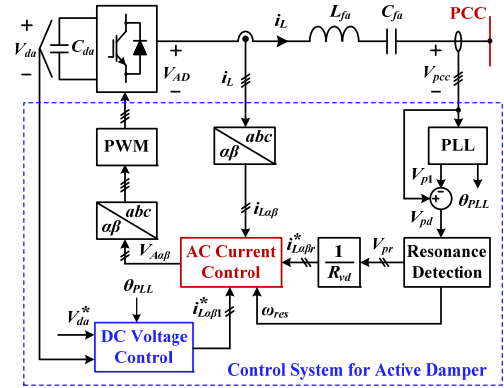


Fig. 2. Overall control of the proposed active damper.

It is therefore non-trivial to design the damper control scheme, whose general representation is provided in Fig. 2.

B. DC-Link Voltage Regulation

DC-link voltage regulation of the damper involves both the DC Voltage Control and AC Current Control blocks shown in Fig. 2. Their purpose is to keep voltage V_{da} across the dc-link capacitor C_{da} constant. Fig. 3 (a) shows a detailed diagram of the DC Voltage Control block, where a Proportional-Integral (PI) controller with the gains of k_{pdc} and k_{idc} has been included for enforcing zero dc voltage error in the steady state. The output of the PI controller is a current command for the ac current control loop, as shown in Fig. 3 (b).

It is important to notice that the control of dc-link voltage is realized by aligning the current command to the orthogonal q -axis of the synchronous reference frame, instead of the d -axis in phase with the PCC voltage. Such a reverse use of current command can be explained by referring to the phasor diagrams at the fundamental frequency, which are drawn in Fig. 4.

First, Fig. 4 shows the allowed region for the fundamental frequency component of the damper current i_{L1} , which can be identified under the following two constraints:

- The voltage magnitude of the damping converter is less than the PCC voltage magnitude, i.e. $|V_{AD1}| < |V_{pcc1}|$.

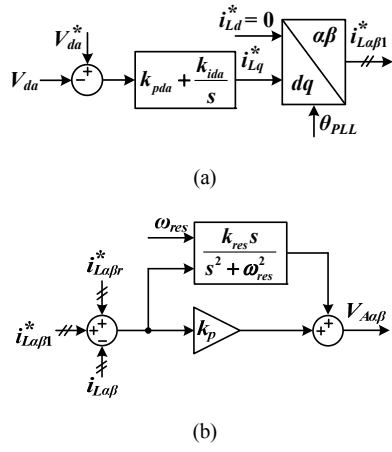


Fig. 3. Block diagram of the (a) DC Voltage Control and (b) AC Current Control blocks of the active damper.

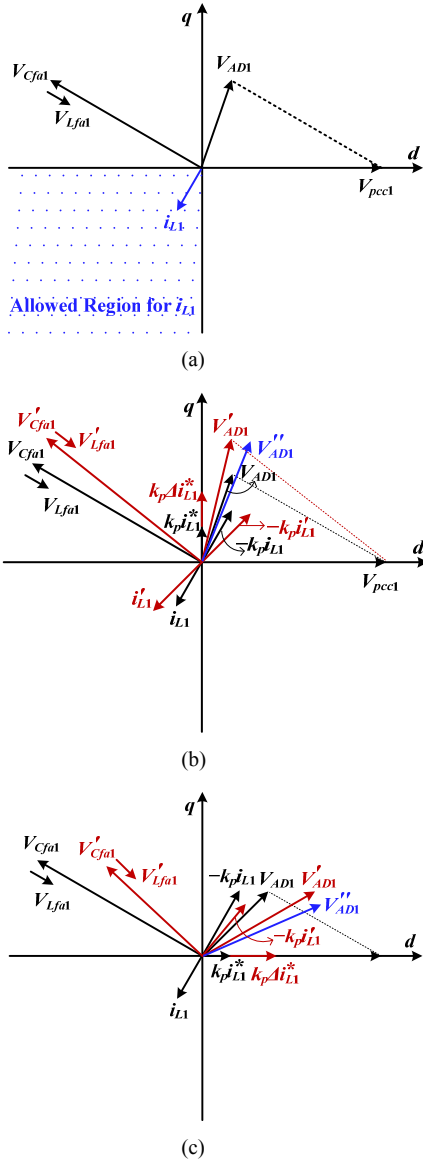


Fig. 4. Phasor diagrams of the active damper. (a) Allowed region for damper current i_L . (b) Current command at q -axis. (c) Current command at d -axis.

- The non-zero active power is absorbed by the damper for compensating the losses.

It is seen that the voltage across the C_{fa} and L_{fa} can only be in the second or third quadrant for meeting $|V_{AD1}| < |V_{pcc1}|$, which implies that i_{L1} is in the third or fourth quadrant. Moreover, the non-zero active power absorbed by the damper means that the actual i_{L1} can only be in the third quadrant and cannot be on the q -axis. It is thus not possible for i_{L1} to track its command with the zero steady-state error, no matter which axis the output of dc-link voltage controller is aligned to. Only a proportional gain k_p is used in Fig. 3 (b) for the fundamental current.

Then, with the proportional current controller, the damper output voltage V_{AD1} can be further decomposed to

$$V_{AD1} = k_p (i_{L1}^* - i_{L1}) \quad (1)$$

where the voltage phasor $k_p i_{L1}^*$ can be aligned to either the d -axis or the q -axis, as shown in Fig. 4 (b) and (c). In the steady-state, the damping converter will absorb reactive power if the current command is aligned along the q -axis, and will generate reactive power if the current command is aligned to the d -axis.

Further on, by considering the dynamic of the dc-link voltage controller, a small disturbance is $k_p \Delta i_{L1}^*$ added to the voltage phasor $k_p i_{L1}^*$ in Fig. 4 (b) and (c). It can be seen that the resulting V_{AD1} rotates back and forth around the steady-state value when $k_p i_{L1}^*$ is aligned along the q -axis, which is shown in Fig. 4 (b). It thus implies a negative feedback control for dc-link voltage. However, it can be seen that the resulting V_{AD1} continuously rotates towards the d -axis when $k_p i_{L1}^*$ is put on the d -axis, as shown in Fig. 4 (c). It indicates an inherent positive feedback control of the dc-link voltage, which destabilizes the system. Therefore, the current command for dc-link voltage regulation can only be put on the q -axis.

C. Resonance Detection and Damping

The Resonance Detection block employs the same method as in the L -filtered active damper [15]. The resonance voltage component is detected by a Pre-filtered Adaptive Notch Filter (P-ANF) based Frequency-Locked Loop (FLL), which is given in Fig. 5. The basic principle underlying this detection scheme is the Least Mean Square (LMS) adaptation algorithm [27]. It is based on the equivalence between the 2-weight LMS-based ANF and Generalized Integrator (GI) [28]. However, unlike the Second-Order GI (SOGI) for grid synchronization [29], the GI is with the sixth-order Taylor series approximation used for the accuracy improvement [30]. Two ANFs are cascaded to form a pre-filtered structure in order to remove the low-order harmonic disturbances on the detection of the high-frequency resonance voltage component [31].

The resonance voltage component is then divided with a chosen virtual resistance R_{vd} for damping purpose. The current command i_{afv}^* is then fed to the AC Current Control block for tracking, which in the stationary frame, can be performed by a GI shown in Fig. 3 (b) with its gain and resonance frequency notated as k_{res} and ω_{res} . It is worth to note that the use of GI is allowed here, because the series LC -filter resonance frequency

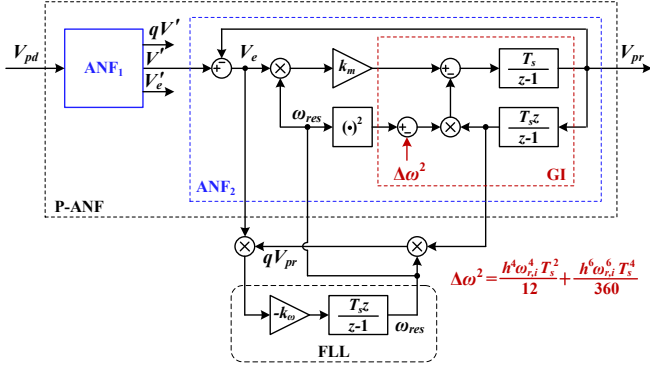


Fig. 5. Block diagram of Resonance Detection block of the active damper.

is lower than the system resonance frequency. Yet it cannot be used to reject the 5th and 7th grid harmonic voltages [26].

III. FREQUENCY-DOMAIN ANALYSIS

To confirm the performance of the damping controller, the damper is modeled in the frequency-domain first, together with only one *LCL*-filtered grid converter in Fig. 1. The impedance-based approach is employed to analyze their interactions under the different grid impedance. Tables I and II list the parameters used for the grid converter and active damper with the control scheme of the former shown in Fig. 6.

Stability of Fig. 6, with its grid current i_2 controlled by a Proportional Resonant (PR) controller in the stationary $\alpha\beta$ -frame, is influenced by the time delay inherited from its digital implementation [32] and the variation of the grid impedance [33]. The active damper is thus added for stabilizing the system by performing the necessary resonance damping.

A. Impedance-Based Model

From Fig. 6, the Norton equivalent model for the current control loop of the grid converter can be derived as follows:

$$Y_m = \frac{i_2}{V_m} \Big|_{V_{pcc}=0} = \frac{Z_{Cf}}{Z_{L1}Z_{L2} + Z_{L2}Z_{Cf} + Z_{Cf}Z_{L1}} \quad (2)$$

$$Y_o = \frac{-i_2}{V_{pcc}} \Big|_{V_m=0} = \frac{Z_{L1} + Z_{Cf}}{Z_{L1}Z_{L2} + Z_{L2}Z_{Cf} + Z_{Cf}Z_{L1}} \quad (3)$$

$$T_c = G_c G_d Y_m, \quad G_{cl} = \frac{T_c}{1 + T_c}, \quad Y_{cl} = \frac{Y_o}{1 + T_c} \quad (4)$$

$$i_2 = G_{cl} i_2^* - Y_{cl} V_{pcc} \quad (5)$$

where Y_m and Y_o characterize the dynamic of the filter “plant” of the current control loop, G_{cl} and Y_{cl} are the closed-loop gain and the closed-loop output admittance, respectively, of the grid current control loop. The Norton equivalent circuit can thus be drawn in Fig. 7 (a) including the grid admittance Y_g . Thus, the influence of the grid impedance on the open-loop gain can

TABLE I
MAIN PARAMETERS OF GRID CONVERTER

Symbol	Quantity	Value
V_g	Grid voltage	400 V
L_g	Grid inductance	0.9 mH
V_{dc}	DC-link voltage	750 V
C_{dc}	DC-link capacitor	340 μ F
L_1	Converter-side filter inductor	2.7 mH
L_2	Grid-side filter inductor	1.8 mH
C_f	Filter capacitor	4.7 μ F
f_{sw}	Switching frequency	10 kHz
T_s	System sampling period	100 μ s
k_{pc}	Proportional current controller	20
k_{rc}	Resonant current controller	600

TABLE II
MAIN PARAMETERS OF PROPOSED ACTIVE DAMPER

Symbol	Quantity	Value
V_{dc}	DC-link voltage	300 V
C_{dc}	DC-link capacitor	1500 μ F
L_{fa}	Series <i>LC</i> -filter inductor	2.7 mH
C_{fa}	Series <i>LC</i> -filter capacitor	10 μ F
f_{sw}	Switching frequency	20 kHz
T_s	System sampling period	50 μ s
k_{pdc}	Proportional gain of dc-link voltage controller	0.5
k_{idc}	Integral gain of dc-link voltage controller	0.01
R_{vd}	Virtual damping resistance	0.2 Ω
k_p	Proportional current controller	15
k_{res}	Resonance damping controller	600
k_{ih}	Proposed integral controller gain	4×10^5
ω_c	Cut-off frequency in the proposed integral controller	250 rad/s

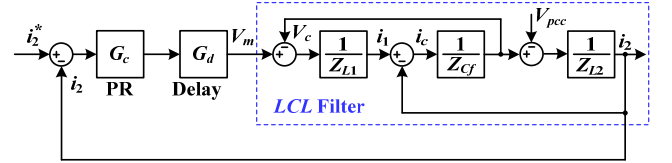


Fig. 6. Grid current control loop for the *LCL*-filtered grid converter.

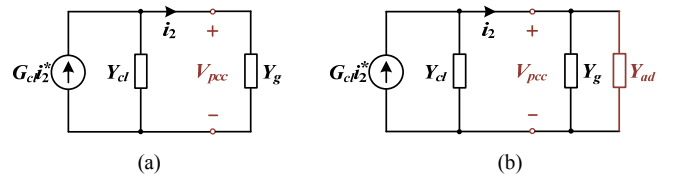


Fig. 7. System equivalent circuit based on the current control loop. (a) Without active damper. (b) With active damper.

be modeled as

$$i_2 = \frac{G_{cl}}{1 + Y_{cl}/Y_g} i_2^* = \frac{T_c}{1 + T_c + Y_{ol}/Y_g} i_2^* \Rightarrow T_{cg} = T_c + Y_{ol}/Y_g \quad (6)$$

Considering then the effect of the active damper, the system

equivalent circuit can be drawn in Fig. 7 (b). The active damper is modeled as the impedance Y_{ad} , whose value is dependent on its current controller and the virtual damping resistance R_{vd} at the resonance frequency. The resulting open-loop gain of the grid current control loop is given by

$$T_{cgd} = T_c + Y_{ol} / (Y_g + Y_{ad}) \quad (7)$$

B. Stability Analysis

Fig. 8 (a) depicts the frequency responses of the open-loop gain of the grid current control loop for the *LCL*-filtered grid converter. Two different grid inductances are evaluated for the stability of the grid converter without using the active damper. It is seen that the current control becomes unstable with a high grid inductance ($L_g = 5$ mH), based on the Nyquist stability criteria. In contrast, in the case of a low grid inductance ($L_g = 0.5$ mH), the system keeps stable because of the inherent damping effect of time delay incurred from the digital control system. In [32], it has been shown that the grid current control loop is stable if the *LCL*-filter resonance frequency is kept lower than the one-sixth of the sampling frequency.

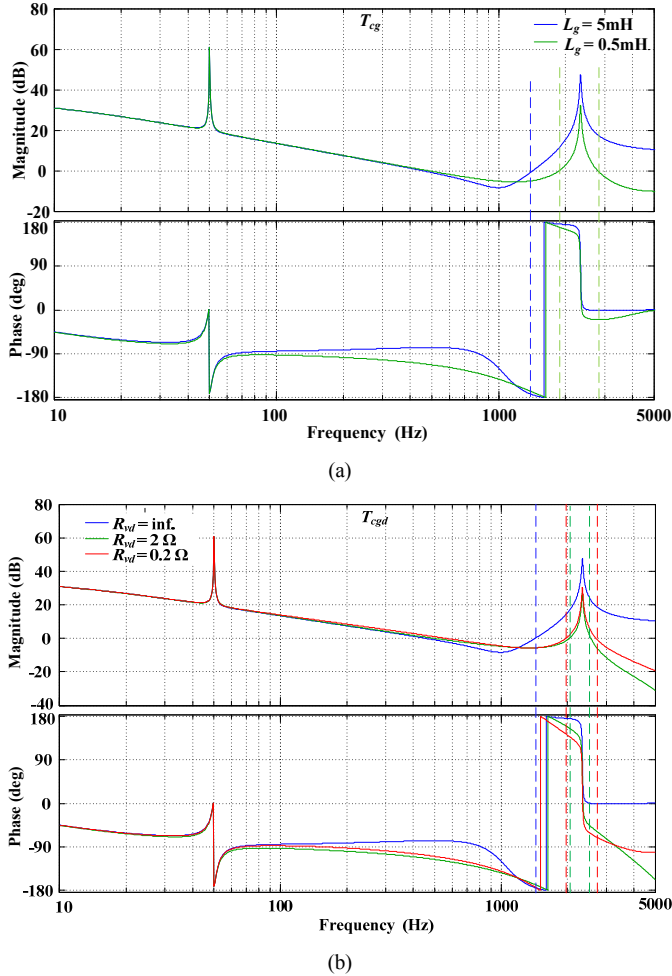


Fig. 8. Frequency responses of the open-loop gains of the grid current control loop. (a) Without active damper. (b) With active damper.

Then, enabling the active damper in the case with the high grid inductance ($L_g = 5$ mH), the frequency responses of the open-loop gain of the grid current control loop are shown in Fig. 8 (b). To evaluate the effects of different virtual damping resistances, a comparison of the frequency responses is made. It clearly shows that with an infinite virtual damping resistance, the system is still unstable, which indicates that zero damping effect is provided by the damper. The smaller virtual resistance makes the damper to provide a better stabilizing performance. This confirms that the active damper can effectively mitigate the influence of grid impedance on the stability of the current control of grid converter.

IV. EXPERIMENTAL RESULTS

To further validate the frequency-domain analysis and the proposed active damper, the three-phase system shown in Fig. 1 is built but with only one *LCL*-filtered grid converter are built and tested based on the parameters given in Tables I and II. The *California Instruments* MX-series AC power supply is used for emulating the ac grid. The control system is built into a *dSPACE* DS1006 system, where the high-speed A/D board, DS2004 is used in synchronism with the digital pulse width modulation board DS5101.

Fig. 9 shows the measured grid current i_2 and its harmonic spectra of the grid converter without the active damper. Two different grid inductances are evaluated. It clearly shows that the converter is unstable in both cases. Also from the harmonic spectra, it can be seen that the resonance frequencies are lower than the one-sixth of the sampling frequency, which matches

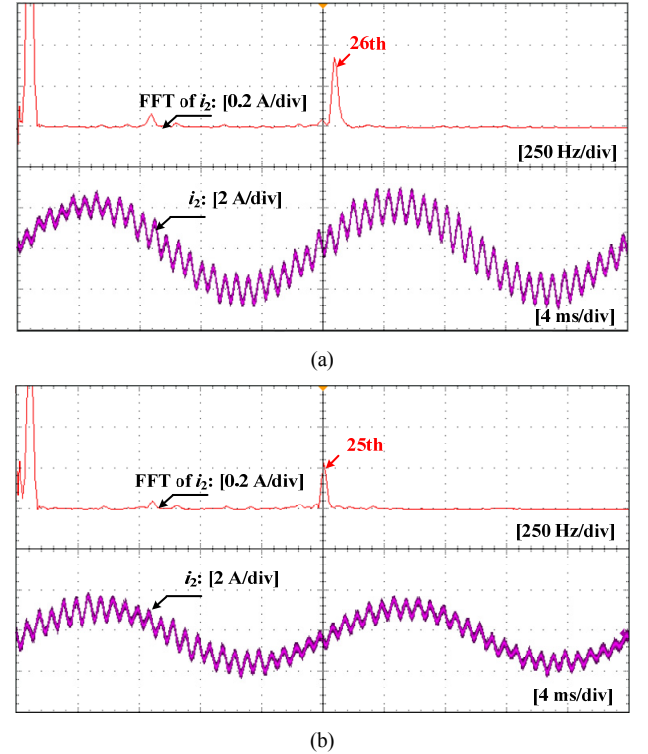


Fig. 9. Measured grid current i_2 of grid-connected converter without active damper and its harmonic spectrum. (a) $L_g = 0.9$ mH. (b) $L_g = 1.8$ mH.

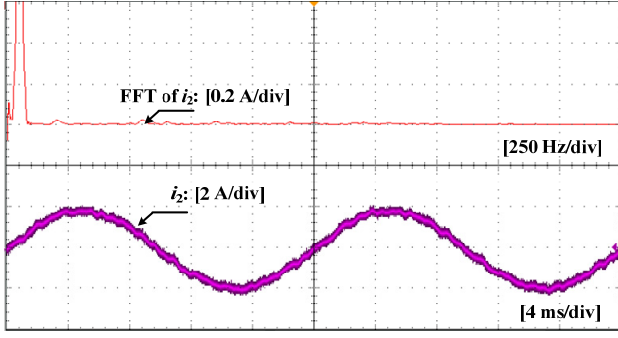
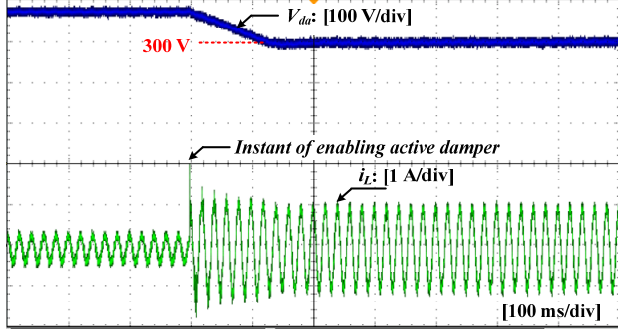
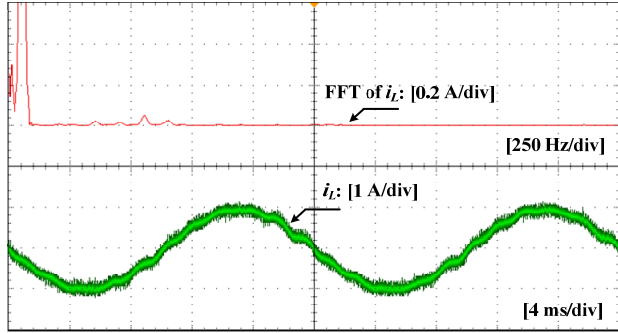


Fig. 10. Measured grid current i_2 of grid-connected converter with enabling the active damper.



(a)



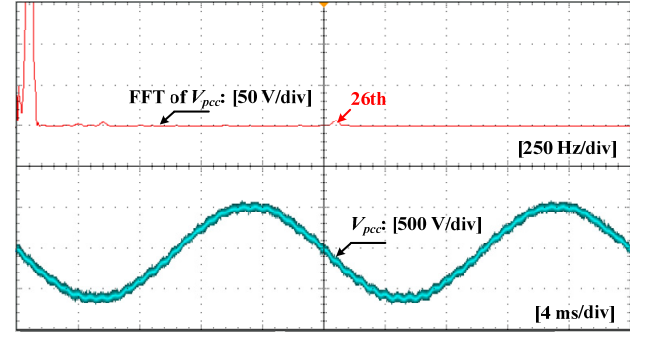
(b)

Fig. 11. Measured dc-link voltage and output current of the active damper. (a) Full view. (b) Zoom-in view of output current.

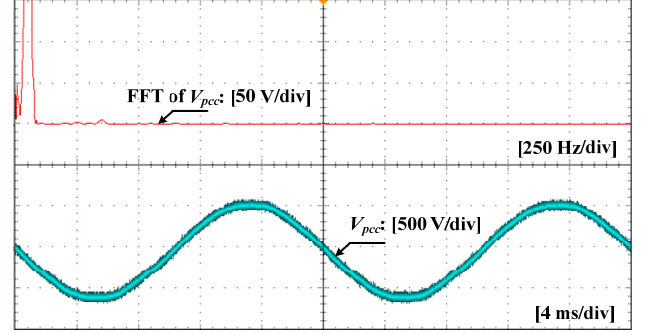
with the stability analysis of grid converter.

Then, adding the damper into the system, the measured grid current and its harmonic spectra for the grid converter is shown in Fig. 10. It is clear that the grid converter becomes stabilized by the active damper, which verifies the effectiveness of the damping control scheme.

Fig. 11 (a) shows the measured dc-link voltage and output current of the active damper. At the instant of enabling the active damper, the dc-link voltage rapidly falls from its pre-charged value (through anti-parallel diodes of the damping converter) to the regulated value of 300 V. Compared with the dc voltage of 750 V needed by the grid converter, the dc-link voltage of the damper is clearly reduced by the added series ac filter capacitor. This voltage reduction can further be increased with a higher rated filter capacitor depending on requirements.



(a)



(b)

Fig. 12. Measured PCC voltage and its harmonic spectra. (a) Without active damper. (b) With active damper.

The zoom-in view of the output current of the active damper is shown in Fig. 11 (b) with its harmonic spectra. The steady-state damper current is used for compensating the losses and absorbing the reactive power, as discussed in Fig. 9.

Fig. 12 shows the measured PCC voltage and its harmonic spectra without and with enabling the active damper. Fig. 12 (a) is corresponding to the unstable case shown in Fig. 10 (a), where a small resonant peak near the 26th harmonic frequency can be observed. Fig. 12 (b) once again confirms the stabilizing effect of the active damper.

V. CONCLUSIONS

This paper presents a series-*LC*-filtered active damper for stabilizing power-electronic-based power systems. It has been experimentally demonstrated that the series ac filter capacitor is able to withstand most of the system voltage. The damping converter can then operate with a low rated voltage, allowing for a faster switching operation. The dc-link voltage regulation through the reactive current command has been clarified. It is found that the usual control of the dc-link voltage by the active current command has a positive feedback mechanism for grid converters connected with a series ac capacitor. Experimental results obtained from a grid converter with the variation of grid impedance has confirmed that the proposed active damper is a promising solution for addressing multiple concerns faced by the modern power systems with a high penetration of power-electronics-based sources and loads.

REFERENCES

- [1] F. Blaabjerg, Z. Chen, and S. B. Kjaer, "Power electronics as efficient interface in dispersed power generation systems," *IEEE Trans. Power Electron.*, vol. 19, no. 5, pp. 1184-1194, Sept. 2004.
- [2] T. M. Jahns and V. Blasko, "Recent advances in power electronics technology for industrial and traction machine drives," *IEEE Proc.*, vol. 89, no. 6, pp. 963-975, Jun. 2001.
- [3] J. H. Enslin and P. J. Heskes, "Harmonic interaction between a large number of distributed power inverters and the distribution network," *IEEE Trans. Power Electron.*, vol. 19, no. 6, pp. 1586-1593, Nov. 2004.
- [4] F. Wang, J. L. Duarte, M. A. M. Hendrix, and P. F. Ribeiro, "Modeling and analysis of grid harmonic distortion impact of aggregated DG inverters," *IEEE Trans. Power Electron.*, vol. 26, no. 3, pp. 786-797, Mar. 2011.
- [5] Z. Shuai, D. Liu, J. Shen, C. Tu, Y. Cheng, and A. Luo, "Series and parallel resonance problem of wideband frequency harmonic and its elimination strategy," *IEEE Trans. Power Electron.*, vol. 29, no. 4, pp. 1941-1952, Apr. 2014.
- [6] X. Wang, F. Blaabjerg, and Z. Chen, "Autonomous control of inverter-interfaced distributed generation units for harmonic current filtering and resonance damping in an islanded microgrid," *IEEE Trans. Ind. Appl.*, vol. 50, no. 1, pp. 452-461, Jan./Feb. 2014.
- [7] X. Wang, F. Blaabjerg, and W. Wu, "Modeling and analysis of harmonic stability in an ac power-electronics-based power system," *IEEE Trans. Power Electron.*, vol. 29, no. 12, pp. 6421-6432, Dec. 2014.
- [8] J. Agorreta, M. Borrega, J. Lopez, and L. Marroyo, "Modeling and control of N -paralleled grid-connected inverters with LCL filter coupled due to grid impedance in PV plants," *IEEE Trans. Power Electron.*, vol. 26, no. 3, pp. 770-785, Mar. 2011.
- [9] P. Brogan, "The stability of multiple, high power, active front end voltage sourced converters when connected to wind farm collector system," in *Proc. EPE WECS 2010*, pp. 1-6.
- [10] L. Harnefors, L. Zhang, and M. Bongiorno, "Frequency-domain passivity-based current controller design," *IET Power Electron.*, vol. 1, no. 4, pp. 455-465, Dec. 2008.
- [11] X. Wang, F. Blaabjerg, and P. C. Loh, "Virtual RC damping of LCL-filtered voltage source converters with extended selective harmonic compensation," *IEEE Trans. Power Electron.*, vol. PP, no. 99, Early Access Article, Oct. 2014.
- [12] R. N. Beres, X. Wang, F. Blaabjerg, C. L. Bak, and M. Liserre, "A review of passive filters for grid-connected voltage source converters," in *Proc. IEEE APEC 2014*, pp. 2208-2215.
- [13] R. N. Beres, X. Wang, F. Blaabjerg, C. L. Bak, and M. Liserre, "Comparative evaluation of passive damping topologies for parallel grid-connected converters with LCL filters," in *Proc. IEEE IPEC 2014*, pp. 3320-3327.
- [14] X. Wang, F. Blaabjerg, M. Liserre, Z. Chen, J. He, and Y. W. Li, "An active damper for stabilizing power-electronics-based AC systems," *IEEE Trans. Power Electron.*, vol. 29, no. 7, pp. 3318-3329, Jul. 2014.
- [15] X. Wang, F. Blaabjerg, and M. Liserre, "An active damper to suppress multiple resonances with unknown frequencies," in *Proc. APEC 2014*, pp. 2184-2191.
- [16] D. Leblanc, B. Nahid-Mobarakeh, B. Pham, S. Pierfederici, and B. Davat, "Stability analysis and active stabilization by a centralized stabilizer of voltage-source-rectifier loads in AC microgrids," in *Proc. IAS 2013*, pp. 1-8.
- [17] H. Akagi, H. Fujita, and K. Wada, "A shunt active filter based on voltage detection for harmonic termination of a radial power distribution line," *IEEE Trans. Ind. Appl.*, vol. 35, no. 3, pp. 638-645, May/Jun. 1999.
- [18] X. Wang, F. Blaabjerg, and Z. Chen, "Synthesis of variable harmonic impedance in inverter-interfaced distributed generation unit for harmonic resonance damping throughout a distribution network," *IEEE Trans. Ind. Appl.*, vol. 48, no. 4, pp. 1407-1417, Jul./Aug. 2012.
- [19] R. Inzunza and H. Akagi, "A 6.6-kV transformerless shunt hybrid active filter for installation on a power distribution system," *IEEE Trans. Power Electron.*, vol. 20, no. 4, pp. 893-900, Jul. 2005.
- [20] L. Harnefors, "Analysis of subsynchronous torsional interaction with power electronic converters," *IEEE Trans. Power Syst.*, vol. 22, no. 1, pp. 305-313, Feb. 2007.
- [21] M. Cespedes and J. Sun, "Modeling and mitigation of harmonic resonance between wind turbines and the grid," in *Proc. IEEE ECCE 2011*, pp. 2109-2116.
- [22] M. Cespedes and J. Sun, "Impedance shaping of three-phase grid-parallel voltage-source converters," in *Proc. IEEE APEC 2012*, pp. 754-760.
- [23] X. Wang, F. Blaabjerg, and P. C. Loh, "Proportional derivative based stabilizing control of paralleled grid converters with cables in renewable power plants," in *Proc. IEEE ECCE 2014*, pp. 4917-4924.
- [24] L. Harnefors, A. G. Yepes, A. Vidal, and J. D. Gandoy, "Passivity-based controller design of grid-connected VSCs for prevention of electrical resonance instability," *IEEE Trans. Power Electron.*, vol. PP, no. 99, Early Access Article, Jul. 2014.
- [25] F. Fuchs and A. Mertens, "Prediction and avoidance of grid-connected converter's instability caused by wind park typical, load-varying grid resonance," in *Proc. IEEE ECCE 2014*, pp. 2633-2640.
- [26] X. Wang, Y. Pang, F. Blaabjerg, and P. C. Loh, "Current control of grid converters connected with series ac capacitor," in *Proc. IEEE APEC 2015*, in press.
- [27] B. Widrow, J. R. Glover Jr., J. M. McCool, J. Kaunitz, C. S. Williams, R. H. Hearn, J. R. Zeidler, E. Dong Jr. and R. C. Googlin, "Adaptive noise canceling: principles and applications," in *Proc. IEEE*, vol. 73, no. 12, pp. 1692-1716, Dec. 1975.
- [28] M. Mojiri, M. Karimi-Ghartemani, and A. Bakhshai, "Estimation of power system frequency using adaptive notch filter," *IEEE Trans. Instrum. Meas.* vol. 56, no. 6, pp. 2470-2477, Dec. 2007.
- [29] A. G. Yepes, F. Freijedo, O. Lopez, and J. Gandoy, "High-performance digital resonant controllers implemented with two integrators," *IEEE Trans. Power Electron.*, vol. 26, no. 2, pp. 563-576, Feb. 2011.
- [30] P. Rodriguez, A. Luna, R. S. Munoz-Aguilar, I. Qadui, R. Teodorescu, and F. Blaabjerg, "A stationary reference frame grid synchronization system for three-phase grid-connected power converters under adverse grid conditions," *IEEE Trans. Power Electron.*, vol. 27, no. 1, pp. 99-112, Jan. 2012.
- [31] J. Matas, M. Castilla, J. Miret, L. G. Vicuna, and R. Guzman, "An adaptive prefiltering method to improve the speed/accuracy tradeoff of voltage sequence detection methods under adverse grid conditions," *IEEE Trans. Ind. Electron.*, vol. 61, no. 5, pp. 2139-2151, May 2014.
- [32] S. G. Parker, B. P. McGrath, and D. G. Holmes, "Regions of active damping control for LCL filters," *IEEE Trans. Ind. Appl.*, vol. 50, no. 1, pp. 424-432, Jan./Feb. 2014.
- [33] X. Wang, F. Blaabjerg, and P. C. Loh, "Analysis and design of grid-current-feedback active damping for LCL resonance in grid-connected voltage source converters," in *Proc. IEEE ECCE 2014*, pp. 373-380.